Biosensors and Bioelectronics 58 (2014) 338–344

Contents lists available at ScienceDirect

Biosensors and Bioelectronics

journal homepage: www.elsevier.com/locate/bios

An integrated giant magnetoimpedance biosensor for detection of biomarker

Tao Wang, Zhen Yang, Chong Lei, Jian Lei, Yong Zhou *

Key Laboratory for Thin Film and Microfabrication of Ministry of Education, Research Institute of Micro/Nano Science & Technology, Shanghai JiaoTong University, Dong chuan Road 800, Shanghai 200240, China

ARTICLE INFO

Article history:
Received 23 December 2013
Received in revised form
3 March 2014
Accepted 3 March 2014
Available online 12 March 2014

Keywords:
Alpha-fetoprotein
Detection
Giant magnetoimpedance
Dynabeads
Au film
Self-assembled monolayer

ABSTRACT

A Dynabeads-labeled magnetic immunoassay (MIA) has been developed by using an integrated giant magnetoimpedance (GMI) biosensor for the detection of alpha-fetoprotein (AFP). The GMI biosensor (Cr/Cu/NiFe/Cu/NiFe/Al_2O_3/Cr/Au films) integrated magnetic sensing elements and a biomolecular immunoplatform. Au film was modified with 11-Mercaptoundecanoic acid (11-MUA) for the immobilization of AFP monoclonal antibody. Double antibody sandwich immunoassay was used to specifically capture and label AFP antigen. Functionalized Dynabeads were conjugated to AFP antigen by streptavidin–biotin binding assay. GMI responses were measured for sensitive detection of AFP from 1 to 10 ng/ml. Our results revealed that the presence of AFP on the biosensor improved the GMI effect owing to the induced magnetic dipole of superparamagnetic Dynabeads, and the GMI ratio was greatly increased at high frequency. Specificity of MIA was tested through the use of 1% bovine serum albumin (BSA). The underlying biophysical mechanisms responsible for the enhanced GMI effect in the detection of AFP were discussed. This work provides a complex lab-on-chip MIA for the detection of biomarker, which may open up a new way for the development of GMI-based MIA in clinical trials.

1. Introduction

In recent years, many efforts have been made to develop a new generation of compact bioanalytical system incorporated with magnetic sensor. Fluxgate sensor (Heim et al., 2009), hall sensor (Lee et al., 2009a), giant magnetoresistance sensor (Pannetier et al., 2011) and spin valve sensor (Ferreira et al., 2002) have been proposed as a biosensor for biomagnetic measurements. Giant magnetoimpedance (GMI) effect has become an interesting topic in magnetic materials research due to its potential for the development of high-performance magnetic sensors (Vacher et al., 2007; Phan and Peng, 2008; Tehranchi et al., 2011; Moulin et al., 2011). GMI effect is the great change of the alternating current (AC) impedance in soft magnetic materials when an external magnetic field is applied (Panina and Mohri, 1994; Panina et al., 1995). In soft magnetic thin films, the GMI effect is caused by the skin effect (Jackson, 1975; Landau and Lifshitz, 1975) as a consequence of the changes in the penetration depth induced by the direct current (DC) applied magnetic field through modification of the transverse permeability (Panina and Mohri, 1994; Panina et al., 1995; Phan and Peng, 2008). This effect has been extensively studied in soft amorphous ferromagnetic wires (Qin et al., 2010; Zhukov et al., 2012), thin films (Zhou et al., 2001; Peksoz et al., 2010; NazariNejad et al., 2013 and ribbons (Phan et al., 2006; Dwevedi and Markandeyulu, 2010; Laurita et al., 2011) for the development of GMI-based sensors in the last decade. GMI sensors have attracted considerable attention because of their several advantages over the conventional magnetic sensors (Ripka et al., 2001; Panina et al., 1995; Phan and Peng, 2008), such as higher sensitivity, smaller size, quicker response and lower cost. The GMI sensors have been introduced into the field of biosensing as a biosensor prototype (Chiriac et al., 2005, 2007; Chiriac and Herea, 2007; Kim et al., 2008; Blanc-Béguin et al., 2009; Yang et al., 2010; Chen et al., 2011) in order to develop a new generation of bioanalytical system.

Magnetic beads have appealed considerable research interest because of their wide applications in magnetic labeling and separation (Sun et al., 2008; Shen et al., 2012; Zhang et al., 2012; Liang et al., 2012; Suaifan et al., 2013; Chen et al., 2013). Dynabeads are uniform polymer spherical magnetic beads that have been made magnetizable and superparamagnetic. Streptavidin-coupled Dynabeads are the gold standard for isolation and handling of biotinylated nucleic acids, antibodies or other biotinylated ligands and targets.

Detection of biomarkers shows great promise for early prediction of related disease. Alpha-fetoprotein (AFP) is a major plasma protein that is produced mainly by the yolk sac and the liver during fetal development. AFP level in serum albumin is related to many diseases, for instance, AFP has been used as a biomarker for monitoring hepatocellular carcinoma, and a raised AFP level is often

* Corresponding author.
E-mail address: yzhou@sjtu.edu.cn (Y. Zhou).

http://dx.doi.org/10.1016/j.bios.2014.03.008
0956-5663/

used in the clinical diagnosis of primary liver cancer (Johnson, 2001). Moreover, elevation of AFP is also used as one factor in the diagnosis of other diseases (Szabó et al., 1990; Johnson, 2001; Rosen and D'Alton, 2005; Taylor and Byrd, 2005; Sturgeon et al., 2009; Krantz et al., 2010). Until now, a variety of methods (Chester et al., 1991; Ito et al., 1999; Lee et al., 2009b; Zhang et al., 2011) have been used for the detection of AFP. However, few works have been done for the detection of AFP using an integrated GMI biosensor.

In the GMI-based biosensing experiment, detection of biological analyte can be realized by measuring the GMI responses of two sets of samples: samples with magnetic-labeled analyte and label-free samples. The functionality basis is supposed to be similar to that proposed earlier for biosensors working on the principle of magnetic field measurements (Baselt et al., 1998; Miller et al., 2002; Kurlyandskaya, 2009): the fringe fields induced by the magnetic particles employed as analyte labels provide a means for transfer of information. In the phase of the analyte detection, the GMI responses are compared for two states: with and without magnetic particles in a tested sample. The differences between the GMI responses can be used to determine the presence, level or absence of the analyte. In this study, an integrated GMI biosensor combined with double antibody sandwich immunoassay was firstly employed to detect AFP. The aim of this study is to explore the possibility and clinical significance of the GMI-based MIA for early diagnosis of cancers.

2. Experimental section

2.1. Reagents

Human AFP antigen, mouse anti-human AFP monoclonal antibody, and Biotinylated mouse anti-human AFP monoclonal antibody were purchased from LNC-Bio (Shanghai Linc-Bio Science Co., Ltd.,). N-Hydroxysuccinimide (NHS) was purchased from Medpep

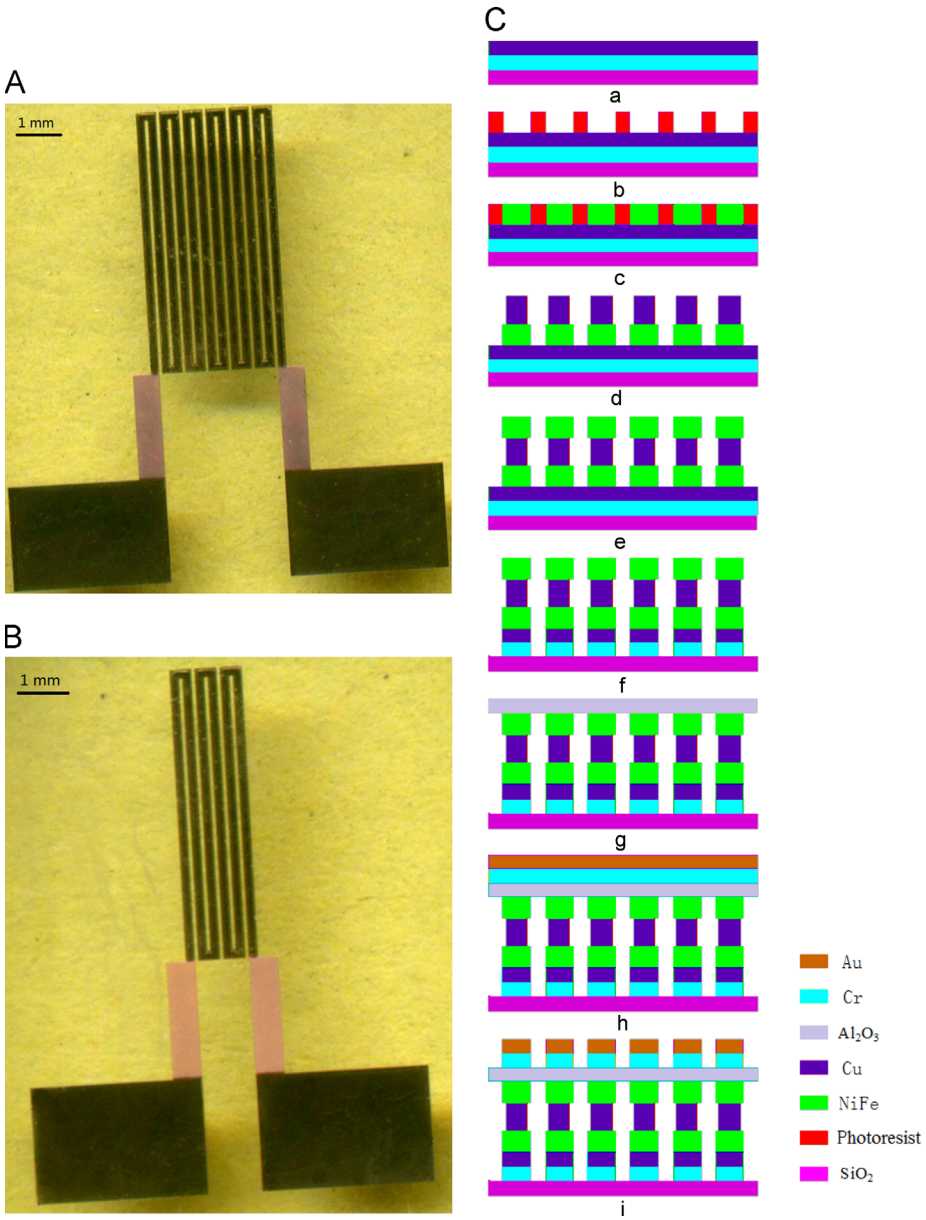

Fig. 1. The integrated GMI biosensor with a meander-line structure. (A) Top view of the sample with 6 turns. (B) Top view of the sample with 3 turns. (C) Illustration of the stepwise process for GMI biosensor fabrication.

(Shanghai Medpep Co., Ltd.,). 11-Mercaptoundecanoic Acid (11-MUA) was purchased from J&K Chemical Ltd.,. (Shanghai, China). 1-ethyl-3-[3-dimethylaminopropyl]carbodiimide (EDC) hydrochloride was purchased from Aladdin Chemistry Co. Ltd., (USA). Phosphate buffer tablets (pH 7.4) were purchased from Medicago AB (Uppsala, Sweden). Dynabeads® MyOne™ Streptavidin C1 were purchased from Invitrogen. Hydrochloric acid (HCl) was purchased from Sinpharm Chemical Reagent Co. Ltd. (Shanghai, China). Sodium hydroxide (NaOH) was purchased from pinghu chemical reagent (Pinghu, China). Bovine serum albumin (BSA) was purchased from wegene (Shanghai, China). Ethanol (CH_3CH_2OH) was purchased from Yangyuan Chemical (Changshu, Co. Ltd.). Acetone (C_3H_6O) was purchased from lingfeng chemical reagent (Shanghai, Co. Ltd.). In the experiments, deionized water was used.

2.2. Instruments

GMI responses were measured by Hewlett-Packard (HP) 4194A. AFP-conjugated Dynabeads were characterized by Scanning Electron Microscopy (SEM) system [ULTRA^{1M} 55, Energy Disperse Spectroscopy (EDS)–INCA PentaFET-x3]. Atomic Force Microscope (AFM) [UHV-SPM] was used for characterization of Au film. Self-assembled monolayer (SAM) was examined by X-ray Photoelectron Spectroscopy (XPS) [AXIS Ultra^{DLD}].

2.3. Design and fabrication of the GMI biosensor

The designed GMI biosensor is composed of Cr/Cu/NiFe/Cu/NiFe/Al_2O_3/Cr/Au films with a meander-line structure. Fig. 1A and B shows the top views of the GMI biosensors. NiFe/Cu/NiFe films were served as GMI sensing elements. Cu film was surrounded by the NiFe films. Au film was used as the biomolecular immunoplatform for double antibody sandwich immunoassay and streptavidin–biotin binding assay. Al_2O_3 film was used as an insulation layer between the sensing elements and the immunoplatform. Transverse and longitudinal directions were defined as that transverse to the straight segment and along the straight segment, respectively. The GMI biosensor was fabricated by Micro-Electro-Mechanical-Systems (MEMS) technology. The fabrication processes (Fig. 1C) were reported in our previous work (Wang et al., 2013). The electroplated NiFe has good soft magnetic properties, which are in accordance with the early reported results (Park and Allen, 2000; Wang et al., 2013). High field sensitivity of GMI can be obtained in sandwich ferromagnetic/conducting/ferromagnetic films with a meander geometrical structure due to the additional inductance from the sample shape (Xiao et al., 1999; Rivero et al., 2003; Wang et al., 2012). Hence, sandwich NiFe/Cu/NiFe films with a meander-line structure were used as GMI sensing elements for biomagnetic measurement in this work.

2.4. Complex immunoassay for capturing and labeling AFP

Dynabeads-labeled immunoassay for AFP was performed on Au film of the GMI biosensor. During the immunoassay, phosphate buffered solution (PBS, pH 7.4) was used as washing liquid. Double antibody sandwich immunoassay and streptavidin–biotin binding assay were employed for the immobilization and labeling of AFP. The immunoassay procedure follows the 8 steps as described below: 1, washing of Au film: the GMI biosensor was incubated in acetone for 15 min, after that it was incubated in 1 M NaOH solution for 10 min and followed by incubation in 1 M HCl solution for 10 min. The GMI biosensor was washed with deionized water and ethanol, then dried in air. 2, 11-MUA served as SAM on Au film: the GMI biosensor was incubated in 30 mmol/l 11-MUA solution at room temperature for 3 h and washed with ethanol, then dried in air. 3, activation of 11-MUA by using EDC and NHS: the GMI biosensor was incubated in the mixture of 200 mM EDC and 50 mM NHS for the activation of 11-MUA at room temperature for 1 h, then washed with PBS for thrice and dried in air. 4, Immobilization of AFP monoclonal antibody: 8 μl of AFP monoclonal antibody with a concentration of 1.06 mg/ml was dropped onto Au film, then the GMI biosensor was incubated at 4 °C for 24 h and then washed with PBS (1% BSA and 0.2% Tween 20) for 5 times. 5, BSA was used to block the nonspecific adsorption sites: the GMI biosensor was incubated in blocking solution (PBS containing 1% BSA) at 4 °C for 2 h, then washed with PBS for 5 times. 6, Immobilization of AFP antigen: 10 μL of AFP antigen with desired concentration was dropped onto Au film, and the GMI biosensor was incubated at room temperature for 1 h and then washed with PBS (1% BSA and 0.2% Tween 20) for 5 times. 7, Immobilization of biotinylated AFP antibody: 6 μL of biotinylated AFP antibody (1 mg/ml) was dropped onto the Au film, and the GMI biosensor was incubated at room temperature for 1 h and then washed with PBS for 5 times. 8, Immobilization of streptavidin-coated Dynabeads: 20 μL of Dynabeads® MyOne™ Streptavidin (10 μg/ml) was dropped onto Au film, and the GMI biosensor was incubated at room temperature for 20 min. Finally, the GMI biosensor was washed with PBS for 5 times. The complex immunoassay is shown in Fig. 2.

2.5. Examination of surface-functionalized Au film

Supplementary information (Figs. S1 and S2, and Tables S1 and S2) shows the Atomic Force Microscope (AFM) characterizations, X-ray Photoelectron Spectroscopy (XPS) measurements, and functional modifications of 11-MUA on Au film. Fig. S1 shows AFM characterizations of Au film and 11-MUA-modified Au film, evidently, the surface morphology of Au film differs from that of 11-MUA-modified Au film. XPS measurements for the 11-MUA are shown in Table S1 (before activation) and Table S2 (after activation). EDC and NHS were used to activate the carboxyl group (COOH) of 11-MUA, and H of COOH would be substituted by N after activation. The functional modification procedure is shown in Fig. S2. It is apparent that S (2p) and C (1 s) account for relatively large proportion after 11-MUA was formed on Au film. The atomic concentration and mass concentration of O (1s) and N (1s) were greatly increased while the atomic concentration and mass concentration of S (2p) and Au (4f) were decreased significantly after activation of 11-MUA. AFM and XPS observations confirm that 11-MUA was well constructed and activated on Au film.

2.6. GMI-based measuring method for the detection of Dynabeads-labeled AFP

The fundamental principle for detection of AFP based on the GMI sensor is that Dynabeads are employed as magnetic labels of AFP antigen, and AFP can be monitored by detecting the fringe

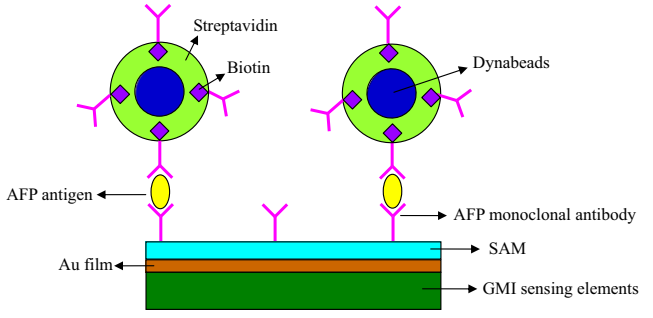

Fig. 2. Complex immunoassay on Au film of the GMI biosensor for capturing and labeling AFP.

field (H_f) of Dynabeads using magnetic sensing elements, as is shown in Fig. 3. During the test, a high-frequency (f) AC (10 mA and 0.1–5 MHz) provided by HP 4194A flowed through the GMI sensor, which produced a transverse AC magnetic field (H_t). A direct current (DC) external magnetic field (H_e) was applied along the longitudinal direction of the sensor in order to induce strong changes in the skin depth. Superparamagnetic beads became strongly magnetized in the presence of H_e and H_t, causing the beads to produce a H_f, thereby modifying superimposed magnetic fields and then altering the magnetoimpedance of the sensing elements. The relative change in impedance (GMI ratio) with H_e was defined as theGMIratio $= 100\% \times [Z(H) - Z(H_0)]/Z(H_0)$, where $Z(H)$ and $Z(H_0)$ were the magnetoimpedance with and without H_e, respectively.

2.7. Characterizations of AFP-conjugated Dynabeads

Dynabeads® MyOne™ Streptavidin C1 are superparamagnetic streptavidin-coated beads with a diameter of 1 μm. SEM images of AFP-conjugated Dynabeads (10 ng/ml and 1 ng/ml) are shown in Fig. 4. It is clear that the numbers of Dynabeads increase with increasing AFP concentration. Elemental analysis of sample was performed by EDS-INCA PentaFET-x3. It is apparent (Table S3) that Fe constitutes a high proportion of elements, which is in accordance with the fact that Fe is the main component of the superparamagnetic Dynabeads. The SEM observations confirm that Dynabeads-labeled AFP was immobilized on Au film of the GMI biosensor.

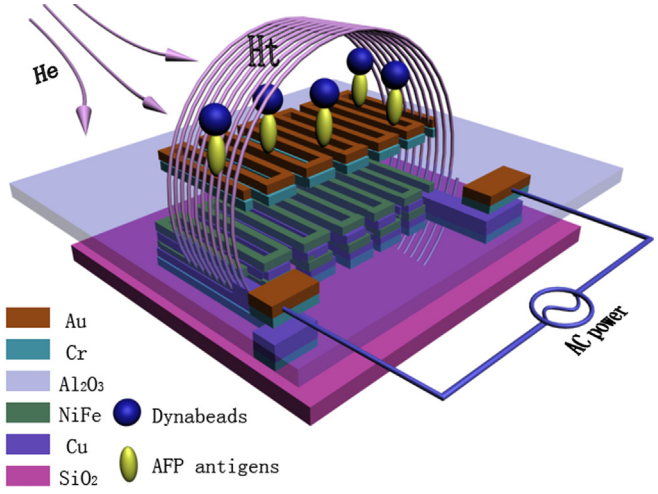

Fig. 3. Double antibody sandwich immunoassay and streptavidin–biotin binding assay were carried out on Au film of the GMI biosensor. Detection of AFP was realized by detecting the magnetic signal of AFP-conjugated Dynabeads.

3. Results and discussion

3.1. Magnetoimpedance measurements for sensitive detection of AFP

In this study, three GMI biosensors (biosensor I, biosensor II and biosensor III) were tested. These GMI biosensors were fabricated by MEMS technology in the same batch of the process. Biosensor I and biosensor III have the same structure (3 number of turns), as shown in Fig. 1B. Biosensor II has the same structure as the other two biosensors except that it has 6 number of turns (see Fig. 1A). Fig. 5A shows the field dependence of the GMI ratio for the biosensor I with and without 10 ng/ml AFP, which are regarded as positive value and negative value, respectively. There is no significant change in the GMI ratio under weak magnetic fields ($<$ 8 Oe) as shown in Fig. 5A, this can be explained by the magnetization rotation model: weak H_e directly determines the low rotational magnetic permeability which is positive correlated with the GMI effect. Furthermore, weak magnetic fields can result in a very low-level magnetization of Dynabeads, and therefore the fringe field is too small to affect the sensing elements. Evidently, the significant change appears in the presence of strong H_e which leads to increased rotational magnetization, and thus resulting in an enhanced GMI effect. The difference between positive value and negative value firstly increases with H_e until the maximum change is obtained near the anisotropy field (Phan and Peng, 2008), then the difference decreases with H_e. This is because the transverse permeability begins to decrease as H_e is further increased, the GMI ratio thereby gradually drops and the impedance becomes independent of stronger H_e. The maximum change of the GMI ratio at f=2 MHz is 8.6% when H_e=24 Oe. Fig. 5B shows the frequency dependence of the GMI ratio for the biosensor I with and without the 10 ng/ml AFP at H_e=24 Oe. Obviously, there is a small change of the GMI ratio at low frequency but large change of the GMI ratio occurs at high frequency as shown in Fig. 5B.

Fig. 5C and D shows the field dependence and the frequency dependence of the GMI ratio for the biosensor II with and without 1 ng/ml AFP, which are regarded as positive value and negative value, respectively. Obviously, the changing trend of the GMI ratio as shown in Fig. 5C is similar to that shown in Fig. 5A, and the GMI ratio increases due to the presence of AFP when H_e is more than 20 Oe. Fig. 5D shows that the GMI ratio is considerably increased in the presence of AFP when 1 MHz $< f <$ 4.5 MHz, and the difference between positive value and negative value firstly increases and then decreases with the increase of frequency. This is because the GMI effect originates mainly from the skin effect owing to a strong change in the effective permeability caused by the applied DC magnetic field. In the case of small skin effect at low frequency, the sensing elements are insensitive to the fringe field, therefore, the GMI biosensor II provides a relatively small change of GMI ratio. The GMI effect is greatly enhanced at high frequency (100 kHz–10 MHz) because both domain wall motion

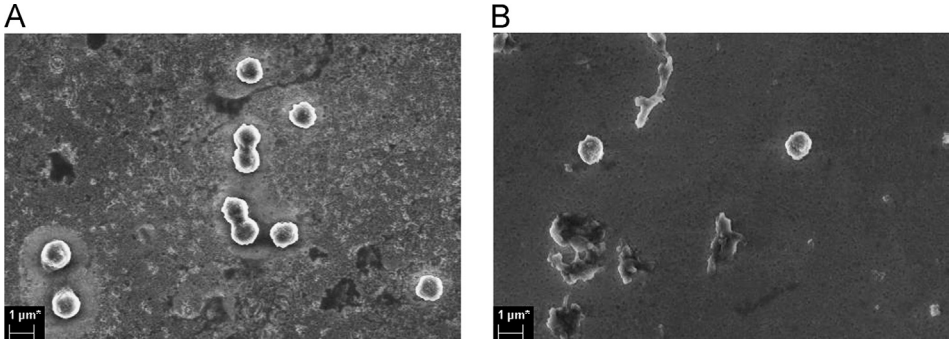

Fig. 4. SEM characterizations of AFP-conjugated Dynabeads at different concentrations (A) 10 ng/ml and (B) 1 ng/ml.

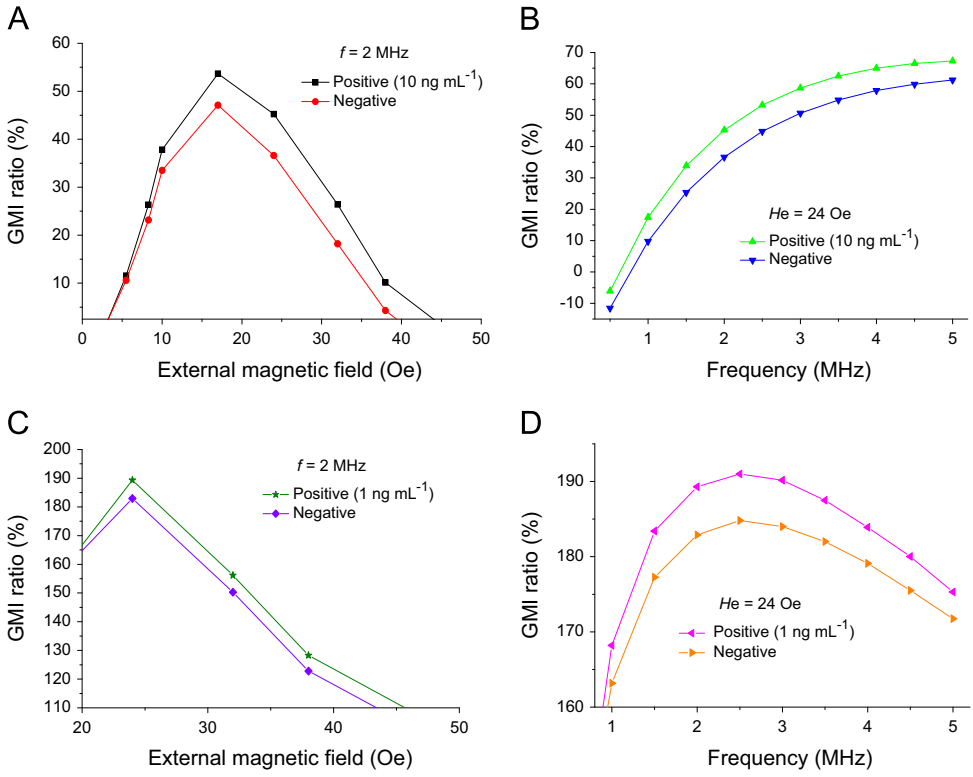

Fig. 5. Results of AFP sensitivity test (A) field dependence of the GMI ratio obtained from biosensor I (10 ng/ml); (B) frequency dependence of the GMI ratio obtained from biosensor I (10 ng/ml); (C) field dependence of the GMI ratio obtained from biosensor II (1 ng/ml); and (D) frequency dependence of the GMI ratio obtained from biosensor II (1 ng/ml).

and magnetic moment rotation contribute to the transverse permeability. This can be understood in terms of derived impedance equation (Phan and Peng, 2008) where the impedance is proportional to the square root of frequency and transverse permeability. In other words, the GMI biosensor II is more sensitive to external magnetic field or fringe field at high frequency. The difference between positive value and negative value begins to go down as frequency is further increased, which is related to domain wall motion damped by the eddy current effect. The greatest change of GMI ratio has taken place near the frequency at which the GMI ratio reaches the maximum, there is an increase of 6.4% at f=2 MHz when H_e=24 Oe.

3.2. Magnetoimpedance measurements for the investigation of specificity

In this case, 1% BSA (PBS solution) served as nonspecific target for testing the specificity of GMI-based MIA with the biosensor III. The whole specificity test was in accordance with that of sensitivity test except that BSA was used instead of AFP antigen. We have carefully examined the surface of biosensor III after specificity test and found that there was only a small quantity of Dynabeads left on the biosensor. The GMI responses of the biosensor III with and without BSA (Blank) are shown in Fig. 6, obviously, there has been a small difference of the GMI ratio between 1% BSA and Blank as shown in Fig. 6. The average change of the GMI ratio is just 2.59% at H_e=24 Oe. In the specificity test, both the field dependence and the frequency dependence of the GMI ratio showed a slight reduction. It is worthwhile to note that there is no positive signal detected after replacing AFP with BSA. The differences of GMI responses between the sensitivity test and the specificity test will be discussed systematically in subsequent chapters.

3.3. Detection limit and linear range

From the viewpoint of immunomagnetic assay, 1 pg/ml AFP with a volume of 10 μL contains about 100,000 AFP molecules, in regard to the immune reaction efficiency, supposing the reaction efficiency is 0.1 in each step, about 100 magnetic beads will be captured on Au film. Moreover, please note that 90 magnetic beads have been detected in our early work (Wang et al., 2013), thus, the expected detection limit will be 1 pg/ml AFP. As you know, the number of magnetic beads is proportional to AFP concentration and thereby the GMI response should be increased with increasing AFP concentration. However, excessively high AFP concentration can result in ferromagnetic effect due to the high-intensity clusters of magnetic beads, which may cause magnetic saturation. Hence, the linear range of GMI responses for AFP detection should be from 1 pg/ml to the magnetic saturation concentration.

3.4. Reproducibility and stability

In order to test the reproducibility of the GMI biosensor for the detection of 10 ng/ml AFP, ten repetitive measurements on one GMI biosensor were performed, which yielded reproducible GMI responses with a relative standard deviation of 1.81%. The study of storage stability demonstrated that the GMI biosensor (10 ng/ml AFP) could retain about 97.2% of its initial response after its storage in the refrigerator at 4 °C for 30 days. The test results indicate that the GMI biosensor exhibits good stability and reproducibility toward detection of AFP.

3.5. Potential biophysical mechanisms and quantitative methods for the detection of biomolecules

It has been observed that AFP-conjugated Dynabeads on the GMI biosensor can give rise to an enhanced GMI effect in the

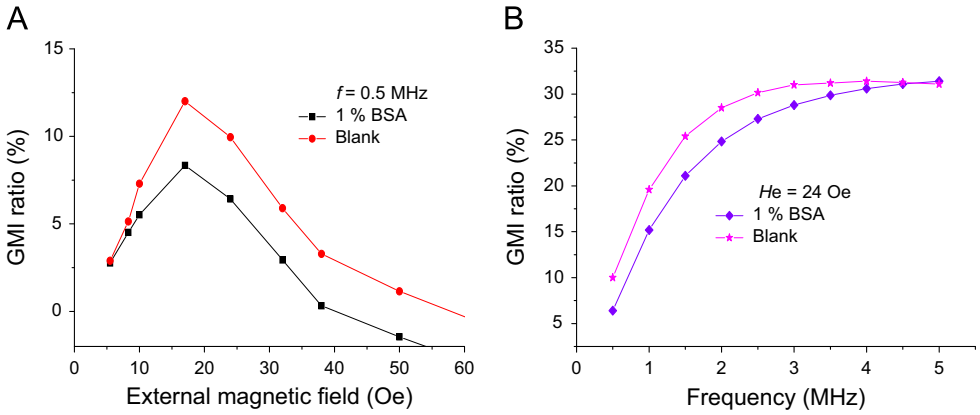

Fig. 6. Biosensor III for testing the specificity of GMI-based MIA by replacing AFP antigen with 1% BSA (A) field dependence of the GMI ratio and (B) frequency dependence of the GMI ratio.

sensitivity test. This phenomenon is consistent with the early reports (Kurlyandskaya and Levit, 2005; Chiriac et al., 2007; Chiriac and Herea, 2007; Yang et al., 2010; Devkota et al., 2013a). Up to now, the physical mechanism of the enhanced GMI effect caused by the magnetic beads is still unclear. Several theories (Kurlyandskaya, 2009; Taysioglu et al., 2009; Peksoz et al., 2010; Laurita et al., 2011; Devkota et al., 2013b) have been proposed to explain the mechanism of the enhanced GMI effect in the presence of coating. Nevertheless, we suggest that the rotational magnetic permeability of the sensing elements is modified by the fringe field, thereby leading to an increase in transverse permeability; thus, magnetic moment rotation is the main contribution to the enhanced GMI effect at high frequency. Further study is needed to better understand the physical origin of the enhanced GMI effect. However, a reverse trend has been observed in the specificity test, namely, the GMI ratio showed a slight reduction at high frequency. Presumably both the Dynabeads distribution and the measurement error lead to this reduction. After careful examination, we found that only a small quantity of Dynabeads was left on the biosensor, and it was distributed mainly near the edge of Au film. This phenomenon could be explained in view of the fact that the immune reaction would not occur by replacing AFP with BSA, thus, the Dynabeads cannot be securely attached to Au film and most of them were washed away by PBS, and only a few Dynabeads were left on the edge of Au film of the biosensor. The Dynabeads may have an edge effect on the sensing elements, this is roughly similar to that of our earlier work (Wang et al., 2013) in which the GMI ratio is greatly reduced since the fringe field appears near the edge of sensing elements.

At present, it is impossible for us to use this lab-on-chip format to perform quantitative detection because the GMI sensors fabricated by electroplating have different GMI properties. In order to quantify the biomarker using different GMI sensors, it is required to have the same GMI properties in fabricated GMI sensors, while there are some problems for us to achieve the uniformity of GMI sensors using the electroplating. Nonuniform solution temperature, external magnetic field and current density are influential factors to film uniformity. Perhaps the difference in magnetic properties of the electroplated NiFe film is the main cause of the difference in the GMI effect. Therefore, the electroplated films always have different GMI properties even if they are in the same batch fabrication. In order to achieve quantitative determination using this lab-on-chip format, we could choose the sputtered magnetic film or amorphous ribbon because they have nearly the same magnetic properties. Previous reports (Devkota et al., 2013a, 2013b; Kurlyandskaya, 2009) about the quantitative analysis of magnetic beads can be used as references for further investigation on the quantification of biomarker. In our early work (Wang et al., 2013), quantitative analysis of Dynabeads was achieved by using a single GMI sensor. Measuring method can be briefly described as that PBS containing magnetic beads with the desired concentration was dropped onto a separate Au film, then the Au film was fixed on a position very close to the GMI sensor for testing. Quantitative determination of magnetic beads was obtained in the linear range of 0.1–5 μg/ml. This method based on the single GMI sensor may also be useful for the quantification of biomarker. In a word, GMI sensor is promising for highly sensitive detection of immunomagnetic bead-labeled biomolecules.

4. Conclusions

In summary, a GMI biosensor was designed, fabricated and tested as an immunosensor prototype, and a GMI-based MIA was developed for the detection of AFP. The GMI biosensor adopted an integrated design for magnetic biosensing and immune reactions. 11-MUA was self-assembled and activated on Au film for the immobilization of AFP monoclonal antibody. Superparamagnetic Dynabeads were conjugated to SAM as the magnetic labels of AFP antigens by double antibody sandwich immunoassay and streptavidin–biotin binding assay. The GMI-based MIA showed high sensitivity and specificity in the detection of AFP, and an enhanced GMI effect was observed due to the bindings of magnetic beads. The results indicate that the GMI biosensor has potential application in the detection of magnetically labeled biomolecules. In future work, investigation on the quantification of biomarker will be carried out by using highly sensitive GMI biosensor.

Acknowledgments

This work was supported by the National Natural Science Foundation of China (Nos. 61074168 and 61273065), the National Science and Technology Support Program (2012BAK08B05), the Natural Science Foundation of Shanghai (13ZR1420800), and the Analytical and Testing Center in Shanghai Jiao Tong University.

Appendix A. Supplementary material

Supplementary data associated with this article can be found in the online version at http://dx.doi.org/10.1016/j.bios.2014.03.008.

References

Baselt, D.R., Lee, G.U., Natesan, M., Metzger, S.W., Sheehan, P.E., Colton, R.J., 1998. Biosens. Bioelectron. 13, 731–739.

Blanc-Béguin, F., Nabily, S., Gieraltowski, J., Turzo, A., Querellou, S., Salaun, P., 2009. J. Magn. Magn. Mater. 321, 192–197.
Chen, L., Bao, C.C, Yang, H., Li, D., Lei, C., Wang, T., Hu, H.Y., He, M., Zhou, Y., Cui, D.X., 2011. Biosens. Bioelectron. 26, 3246–3253.
Chen, Y.Y., Cheng, H.W., Tram, K., Zhang, S.F., Zhao, Y.H., Han, L.Y., Chena, Z.P., Huan, S.Y., 2013. Analyst 138, 2624–2631.
Chester, S.J., Maimonis, P., Vanzuiden, P., Finklestein, M., Bookout, J., Vezeridis, M.P., 1991. Dis. Markers 9, 265–271.
Chiriac, H., Tibu, M., Moga, A., Herea, D., 2005. J. Magn. Magn. Mater. 293, 671–676.
Chiriac, H., Herea, D., Corodeanu, S., 2007. J. Magn. Magn. Mater. 311, 425–428.
Chiriac, H., Herea, D., 2007. Int. J. Appl. Electromagn. Mech. 25, 453–459.
Dwevedi, S., Markandeyulu, G., 2010. J. Appl. Phys. 107, 09A328.
Devkota, J., Wang, C., Ruiz, A., Mohapatra, S., Mukherjee, P., Srikanth, H., Phan, M.H., 2013a. J. Appl. Phys. 113, 104701.
Devkota, J., Ruiz, A., Mukherjee, P., Srikanth, H., Phan, M.H., 2013b. IEEE Trans. Magn. 49, 4060–4063.
Ferreira, H.A., Graham, D.L., Freitas, P.P., Cabral, J.M.S., 2002. J. Appl. Phys. 93, 7281–7286.
Heim, E., Ludwig, F., Schilling, M., 2009. J. Magn. Magn. Mater. 321, 1628–1631.
Ito, K., Oda, M., Tsuji, A., Maeda, M.J., 1999. J. Pharm. Biomed. Anal. 20, 169–178.
Jackson, J.D., 1975. Classical Electrodynamics. John Wiley &Sons, Inc., USA.
Johnson, P.J., 2001. Clin. Liver Dis. 5, 145–159.
Kim, D., Kim, H., Park, S., Lee, W., Jeung, W.Y., 2008. IEEE Trans. Magn. 44, 3985–3988.
Krantz, D.A., Hallahan, T.W., Sherwin, J.E., 2010. Clin. Lab. Med. 30, 721–725.
Kurlyandskaya, G.V., Levit, V., 2005. Biosens. Bioelectron. 20, 1611–1616.
Kurlyandskaya, G.V., 2009. J. Magn. Magn. Mater. 321, 659–662.
Lee, W., Joo, S.J., Sun, U.K., Rhie, K.W., Hong, J.K., Shin, K.H., Kim, K.H., 2009a. Appl. Phys. Lett. 94, 153903.
Lee, Y.M., Jeong, Y., Kang, H.J., Chung, S.J., Chung, B.H., 2009b. Biosens. Bioelectron. 25, 332–337.
Landau, L.D., Lifshitz, E.M., 1975. Electrodynamics of Continuous Media. Pergamon Press, Oxford
Laurita, N., Chaturvedi, A., Bauer, C., Jayathilaka, P., Leary, A., Miller, C., Phan, M.H., McHenry, M.E., Srikanth, H., 2011. J. Appl. Phys. 109, 07C706.
Liang, R.P., Yao, G.H., Fan, L.X., Qiu, J.D., 2012. Anal. Chim. Acta 737, 22–28.
Miller, M.M., Prinz, G.A., Cheng, S.F., Bounnak, S., 2002. Appl. Phys. Lett. 81, 2211–2213.
Moulin, J., Shahosseini, I., Alves, F., Mazaleyrat, F., 2011. J. Micromech. Microeng. 21, 074010–074017.
NazariNejad, S., Fomani, A.A., Mansour, R., 2013. IEEE Trans. Magn. 49, 3874–3877.
Panina, L.V., Mohri, K., 1994. Appl. Phys. Lett. 65, 1189–1191.
Panina, L.V., Mohri, K., Uchiyama, T., Noda, M., 1995. IEEE Trans. Magn. 31, 1249–1260.
Pannetier, L.M., Parkkonen, L., Sergeeva, C.N., Polovy, H., Fermon, C., Fowley, C., 2011. Appl. Phys. Lett. 98, 153705.
Park, J.Y., Allen, M.G., 2000. IEEE Trans. Electron. Packag. Manuf. 23, 48.
Peksoz, A., Kaya, Y., Taysioglu, A.A., Derebasi, N., Kaynak, G., 2010. Sensors Actuators A 159, 69–72.
Phan, M.H., Peng, H.X., Wisnom, M.R., Yu, S.C., Nghi, N.H., Kim, C.G., 2006. Sensors Actuators A 129, 62–65.
Phan, M.H., Peng, H..X., 2008. Prog. Mater. Sci. 53, 323–420.
Qin, F.X., Peng, H.X., Phan, M.H., 2010. Mater. Sci. Eng. 167, 129–132.
Ripka, P., Kraus, L., Ripka, P., 2001. Magnetic Sensors and Magnetometers. Artech House, Boston, pp. 350–358
Rivero, M.A., Maicas, M., Lopez, E., Aroca, C., Sanchez, M.C., Sanchez, P., 2003. J. Magn. Magn. Mater. 636, 254–255.
Rosen, T., D'Alton, M.E., 2005. Semin. Perinatol. 29, 367–375.
Shen, L.p., Zhang, X.L., Jin, W.R., 2012. Analyst 137, 4849–4854.
Sturgeon, C.M., Lai, L.C., Duffy, M.J., 2009. BMJ 339, b3527.
Suaifan, G.A., Esseghaier, C., Ng, A., Zourob, M., 2013. Analyst 138, 3735–3739.
Sun, Y., Bi, N., Song, D.Q., Bai, Y., Wang, L.Y., Zhang, H.Q., 2008. Anal. Chim. Acta 624, 294–300.
Szabó, M., Veress, L., Münnich, A., Papp, Z., 1990. Orv Hetil 131, 2139–2142.
Taylor, A.M., Byrd, P.J., 2005. J. Clin. Pathol. 58, 1009–1015.
Taysioglu, A.A., Peksoz, A., Kaya, Y., Derebasi, N., Irez, G., Kaynak, G., 2009. J. Alloys Compd. 487, 38–41.
Tehranchi, M.M., Ranjbaran, M., Eftekhari, H., 2011. Sensors Actuators A 170, 55–61.
Vacher, F., Alves, F., Gilles, C., 2007. NDT & E Int. 40, 439–442.
Wang, T., Zhou, Y., Lei, C., Lei, J., Yang, Z., 2012. Appl. Phys. A 109, 205–211.
Wang, T., Zhou, Y., Lei, C., Lei, J., Yang, Z., 2013. Sensors Actuators B 186, 727–733.
Xiao, S.Q., Liu, Y.H., Dai, Y.Y., Zhang, L., 1999. J. Appl. Phys. 85, 4127–4130.
Yang, H., Chen, L., Lei, C., Zhang, J., Li, D., Zhou, Z., Bao, C.C, Hu, H., Chen, X., Cui, F., 2010. Appl. Phys. Lett. 97, 043702.
Zhang, Y., Ge, S., Wang, S., Yan, M., Yu, J., Song, X., Liu, W., 2012. Analyst 137, 2176–2182.
Zhang, B., Tang, D., Liu, B., Chen, H., Cui, Y., Chen, G., 2011. Biosens. Bioelectron. 28, 174–180.
Zhou, Y., Yu, J.Q., Zhao, X.L., Cai, B.C., 2001. J. Appl. Phys. 89, 1816–1819.
Zhukov, A., Ipatov, M., Blanco, J.M., Zhukova, V., 2012. Open Mater. Sci. J. 6, 39–43.